International Journal of Nanomedicine

Dovepress
Taylor & Francis Group

Open Access Full Text Article

ORIGINAL RESEARCH

Conglomerated Imiquimod and Metronidazole Incorporated Biodegradable Nanofibrous Mats for Potential Therapy of Cervical Cancer

Yi-Pin Chen[1,2], Chiao-Fan Chiu[3,4], Chien-Neng Wang[1], Chu-Chi Lin[1], Chia-Rui Shen[5–7], Yi-Chen Yao[8], Yi-Hua Kuo[8], Shih-Jung Liu[8,9]

[1]Department of Obstetrics and Gynecology, Keelung Chang Gung Memorial Hospital, Keelung, 20401, Taiwan; [2]School of Traditional Chinese Medicine, College of Medicine, Chang Gung University, Taoyuan, Taiwan; [3]Department of Pediatrics, Linkou Medical Center, Chang Gung Memorial Hospital, Taoyuan, 333, Taiwan; [4]Graduate Institute of Clinical Medical Sciences, College of Medicine, Chang Gung University, Taoyuan, 33302, Taiwan; [5]Department of Medical Biotechnology and Laboratory Science, Chang Gung University, Taoyuan, 33302, Taiwan; [6]Department of Ophthalmology, Lin-Kou Chang Gung Memorial Hospital, Taoyuan, Taiwan; [7]R&D Center of Biochemical Engineering Technology, Department of Chemical Engineering, Ming Chi University of Technology, New Taipei, Taiwan; [8]Department of Mechanical Engineering, Chang Gung University, Taoyuan, 33302, Taiwan; [9]Bone and Joint Research Center, Department of Orthopedic Surgery, Chang Gung Memorial Hospital-Linkou, Taoyuan, 33305, Taiwan

Correspondence: Shih-Jung Liu, Department of Mechanical Engineering, Chang Gung University, 259, Wen-Hwa 1st Road, Kwei-Shan, Tao-Yuan, 33302, Taiwan, Tel +886-3-2118166, Fax +886-3-2118558, Email shihjung@mail.cgu.edu.tw

Background: In clinical practice, imiquimod is used to treat Human Papillomavirus (HPV)-related lesions, such as condyloma and Cervical Intraepithelial Neoplasia (CIN). Metronidazole is the most commonly prescribed antibiotic for bacterial vaginosis. The study developed biodegradable imiquimod- and metronidazole-loaded nanofibrous mats and assessed their effectiveness for the topical treatment of cervical cancer, a type of HPV-related lesion.

Methods: Nanofibers of two distinct poly[(d,l)-lactide-*co*-glycolide] (PLGA)-to-drug ratios (6:1 and 4:1) were manufactured through the electrospinning technology. The in vitro release behavior of imiquimod and metronidazole was evaluated via an elution method, while the in vivo discharge behavior was evaluated on a mice model. Additionally, a model of cervical cancer was established using C57BL/6J mice, and it was utilized to evaluate the efficacy of drug-eluting nanofibers through in vivo testing. Mice afflicted with cervical cancer were separated into three distinct groups for the study: The mice in Group A served as the control and received no treatment. Group B received treatment with pure PLGA nanofibers (no drugs loaded), whereas Group C received treatment with nanofibers loaded with imiquimod and metronidazole. Post implantation, the variations in tumor sizes of rats receiving the implantation of drug-eluting nanofibers were monitored.

Results: The experimental data show that drug-eluting nanofibers could discharge in vitro high concentrations of imiquimod and metronidazole for exceeding 30 days. In vivo, each membrane consistently released elevated concentrations of imiquimod/metronidazole at the intended site in mice over a four-week period, with minimal systemic drug concentration detected in the bloodstream. The mice treated with drug-loaded nanofibers displayed noticeably reduced tumor volumes compared to both the control group and the group treated with pristine nanofibers. Histological examination revealed the absence of any discernible tissue inflammation.

Conclusion: Biodegradable nanofibers with a sustainable release of imiquimod and metronidazole demonstrated their effectiveness and lasting impact of treating mice with cervical cancer.

Keywords: cervical cancer, degradable nanofibers, imiquimod, metronidazole, extended drug release

Introduction

Cervical carcinoma is one of the most common gynecological cancers worldwide, accounting for approximately 12% of all carcinomas in women.[1] It originates from abnormal cell growth in the cervix and has the potential to invade or metastasize to other parts of the body. In the early stages, cervical carcinoma often presents no noticeable symptoms, but as it progresses, it may cause abnormal vaginal bleeding, pelvic pain, or pain during sexual intercourse. Although postcoital bleeding is common, it can also be an indicator of cervical cancer.[2,3]

Received: 14 August 2024
Accepted: 15 January 2025
Published: 21 January 2025

The primary risk factor for the development of cervical intraepithelial neoplasia and cervical cancer is infection with the human papillomavirus (HPV).[4] Over 30 hPV types can infect the genital tract, and certain high-risk strains are strongly linked to cervical cancer. More than 99% of cervical carcinoma cases are associated with HPV infection, underscoring its critical role as a primary risk factor. While HPV infection is present in over 90% of cases, not all HPV-infected individuals develop cervical cancer.[5] Other contributing risk factors include smoking, the use of oral contraceptives, and early sexual activity. The transition from precancerous changes to cervical cancer usually takes 10 to 20 years. Squamous cell carcinoma is the most common type, comprising about 69% of cases, followed by adenocarcinoma at 25%, with other types being rare. Diagnosis typically involves cervical biopsy and medical imaging.[6]

While prophylactic HPV vaccines can prevent up to 90% of cervical cancer cases, it is still recommended to undergo regular Pap smears, limit the number of sexual partners, and use condoms. Pap smears and cervical biopsies are essential for diagnosing cervical intraepithelial neoplasia (CIN), a precursor to cervical cancer.[7] Treatment options may include surgical procedures, chemotherapy, and/or radiotherapy, either alone or in combination. Factors such as tumor budding, cell nest size, depth of stromal invasion, lymphovascular space invasion, perineural invasion, tumor-free distance, and tumor-infiltrating lymphocytes are important for assessing the prognosis of cervical cancer and warrant further investigation.[8,9] However, despite these interventions, many women succumb to cervical cancer each year. There is a pressing need for the development of new therapeutic approaches to better manage this devastating disease.

To date, scientists have engineered nanofibrous mats infused with various compounds, such as cisplatin and curcumin,[10] dichloroacetate (DCA) and oxaliplatin,[11] Pt(IV) prodrug-based micelles,[12] and andrographolide-embedded nanofibers,[13] aimed at reducing tumor recurrence in cervical cancer therapy. Experimental findings indicate that these implanted devices demonstrate enhanced anticancer effectiveness while exhibiting reduced systemic toxicity in vivo against advanced cervical cancer.

In this study, we exploited degradable imiquimod- and metronidazole-loaded nanofibers as an anticancer film to provide sustained, topical release of anticancer drugs at the target area to inhibit the progression of cervical cancer. Imiquimod serves as an immune response modifier medication utilized in the treatment of genital warts, superficial basal cell carcinoma, and actinic keratosis.[14,15] Its potent antitumoral effects are achieved through synergistic actions across various immunological pathways. Imiquimod activates toll-like receptor 7 (TLR7), a key player in pathogen recognition, thereby stimulating the innate immune system. Cells activated by imiquimod release cytokines, notably interferon-α (IFN-α), interleukin-6 (IL-6), and tumor necrosis factor-α (TNF-α). Topical application of imiquimod has been shown to activate Langerhans cells, which subsequently migrate to local lymph nodes, activating the adaptive immune system.[16] Additionally, other immune cell types, including natural killer cells, macrophages, and B-lymphocytes, are also activated by imiquimod. Clinical studies have shown that local application of imiquimod is safe and effective for the off-label treatment of HPV-related lesions and HPV elimination.[17]

In contrast, metronidazole functions as an antibiotic and antiprotozoal medication. It is employed either alone or in combination with other antibiotics for the treatment of pelvic inflammatory disease, endocarditis, and bacterial vaginosis.[18] Metronidazole demonstrates efficacy against dracunculiasis, giardiasis, trichomoniasis, and amebiasis. Furthermore, it serves as an option for managing a first episode of mild-to-moderate Clostridium difficile colitis when vancomycin or fidaxomicin is not available.[19]

The combined use of imiquimod and metronidazole offers promising benefits for treating cervical cancer, particularly in localized or early-stage cervical lesions. Imiquimod combats HPV-related immune evasion, while metronidazole targets microbial factors that can exacerbate inflammation and contribute to tumor progression. Together, they reduce local infections and inflammation (via metronidazole) while enhancing immune responses (via imiquimod), creating a less favorable environment for tumor growth. By addressing both HPV infection and inflammation, this combination may also help reduce the risk of recurrence after treatment.

To fabricate the degradable nanofibrous membranes, a mixture comprising imiquimod, metronidazole, and poly[(d,l)-lactide-co-glycolide] (PLGA) was combined with hexafluoro-2-propanol (HFIP) and processed via electrospinning to produce nanofibrous mats. Spun nanofibrous mats were evaluated by scanning electron microscopy (SEM), tensile tester, water contact angle analyzer, and Fourier-transform infrared spectroscopy (FTIR). The in vitro discharge pattern of imiquimod and metronidazole from the nanofibers was explored by an elution scheme and a high-performance liquid

chromatography (HPLC) analysis. The in vivo discharge profile was evaluated on a mice model. Histological analysis was also completed.

Materials and Methods

Preparation of Imiquimod and Metronidazole Incorporated Nanofibers

The degradable polymeric material utilized was PLGA (LA:GA=50:50) (Sigma-Aldrich, St. Louis, Mo, USA) that has a molecular weight of 24–38 kDa. The pharmaceuticals adopted included imiquimod and metronidazole, both were purchased from Sigma-Aldrich.

Nanofibrous membranes with two different PLGA-to-imiquimod/metronidazole ratios, specifically 6:1 and 4:1, were created using an electrospinning apparatus.[20] For the production of nanofibrous membranes with a 6:1 polymer-to-drug ratio, a mixture of PLGA, imiquimod, and metronidazole (1200 mg/100 mg/100 mg) was initially blended with 5 mL of hexafluoro-2-propanol (HFIP) (Sigma-Aldrich) using a stirrer for 4 hours. This mixture was fed into the electrospinning setup using a syringe pump at a flow rate of 0.7 mL/h, and after 6 hours of spinning, it resulted in the formation of nonwoven nanofibrous membranes on a grounded aluminum plate under ambient conditions of 25°C and 75% relative humidity. The needle used in the experiments has an internal diameter of 413 μm (22 Gauge). The voltage was adjusted to 17 kV, while maintaining a distance of 15 cm between the needle and the aluminum plate. To produce nanofibers with a 4:1 polymer-to-drug ratio, the spinning process was replicated, with the only variation being the polymer/imiquimod/metronidazole ratio, which was adjusted to 1120 mg/140 mg/140 mg. Additionally, the flow rate of the syringe pump was set to 0.5 mL/h.

Assessment of Electrospun Nanofibers

The spun nanofibers underwent evaluation using an SEM (Joel JSM-7500F, Tokyo, Japan). Fifty randomly selected nanofibers from each microimage were used to determine the distribution of fiber diameters (n=5).

To evaluate the wetting capability of the spun membranes, a contact angle measurement device (First Ten Angstroms, USA) (n= 5) was employed. Test specimens measuring 1.0 cm x 1.0 cm were extracted from the nanofibrous membranes and positioned on a testing plate. Distilled water was then meticulously dripped onto the surfaces of the specimens. Wetting angles were captured using a video monitor.

Tensile properties of the nanofibrous membranes were determined using a Lloyd tensiometer (Ametek, U.S.A.). A membranous strip measuring 10 mm x 50 mm was secured between two clamps positioned 3 cm apart. The strip was then pulled by one clamp at a rate of 60 mm per minute over a distance of 10 cm before returning to its initial position. The ultimate tensile strength and fracture strain were recorded (n=5).

A FTIR spectrometry (Thermo Scientific Model Nicolet iS5 spectrometer) was utilized to investigate the spectra of electrospun pure PLGA and imiquimod/metronidazole loaded PLGA nanofibers. Samples were pressed into KBr discs. The spectra were observed in absorption modes at resolutions of 4 cm^{-1} with 32 scans across the 400–4000 cm^{-1} range.

In-vitro Release Characterization

The in vitro release profiles of imiquimod and metronidazole from the drug-loaded nanofibrous mats with different PLGA-to-drug ratios (6:1 and 4:1) were determined using the elution method. Samples measuring 10 mm × 10 mm and weighing 3 mg were immersed in 1 mL of buffered solution. After incubating in an isothermal oven at 37°C for 24 hours, the eluent was collected and analyzed. The phosphate buffer was replaced every 24 hours, and this process was repeated for a duration of 30 days.

The imiquimod levels were characterized by a HPLC analysis conducted on a Hitachi L-2200R system (Tokyo, Japan), employing a Inertsil C18 (250 mm x 4.6 mm, 5 um particle size) column.[21] The column temperature was kept at 40°C. The mobile phase consisted of 0.01 M Phosphate monobasic+0.1% Triethylamine/Ortho-phosphoric acid (to pH 2.46) (70%) and acetonitrile (30%). Absorbance was measured at a wavelength of 254 nm. The volumetric flow rate was set at 1.4 mL/min, with a retention time of 10 mins. Meanwhile, the same column with the temperature maintained at

25°C was utilized for the analysis of metronidazole. The mobile phase included phosphate buffered solution (pH 7) (70%) and acetonitrile (30%). The absorbency used was 319 nm and the volumetric flow rate was 1.0 mL/min.[22]

Cell Line, Antibodies, and Peptides

The TC-1 cell line is a well-known cancer cell line derived from lung epithelial cells that have been genetically modified to express the carcinogenic E6 and E7 genes of the human papillomavirus (HPV). It is frequently used in preclinical research on HPV-associated malignancies and lung cancers. These cells are highly carcinogenic and provide a valuable model for studying immune responses, tumor progression, and potential therapeutic interventions. TC-1 cells are particularly useful for researching immunotherapeutic treatments and exploring the impact of HPV on lung cancer development.

For this study, the HPV-positive, E7-expressing tumorigenic TC-1 cell line was obtained from Dr. T.C. Wu at Johns Hopkins University, USA. The use of this cell line was approved by the institutional review board.[13] On day 0, mice were subcutaneously injected in the back region with 2×10^5 HPV+ TC-1 tumor cells per mouse. The TC-1/luc cells were isolated from C57BL/6 primary lung epithelial cells and transformed with human papillomavirus (HPV) type-16, E6, E7 oncogenes, and activated H-ras.[23] The TC-1 cells were cultured in RPMI-1640 medium (Invitrogen) supplemented with 10% fetal bovine serum (Invitrogen) and 0.2 μg/mL puromycin. The HPV16 E7 MHC class I and II peptides were acquired from Sigma Chemical Co. (St. Louis, MO, USA) at a purity of ≥95%. Mouse IFN-γ was purchased from Biolegend (San Diego, CA, USA).

In vivo Animal Study

All animal procedures were approved by the Institutional Animal Care and Use Committee (IACUC) of Chang Gung University (Approval No.: CGU-108-108, 108-168). The experiments were conducted in compliance with the regulations of the National Institutes of Health of Taiwan and under the supervision of a licensed veterinarian. Mice were anesthetized with isoflurane delivered via inhalation through an atomizer in a transparent chamber (40×20×28 cm). After shaving, an incision was made on the backs of the mice to expose the tissues (Figure 1A). Surgery was performed while maintaining anesthesia with continuous isoflurane inhalation through a mask. Following the implantation of PLGA nanofibrous mats with a 4:1 polymer-to-drug ratio (Figure 1B), the incision was closed with 3–0 Vicryl sutures (Figure 1C).

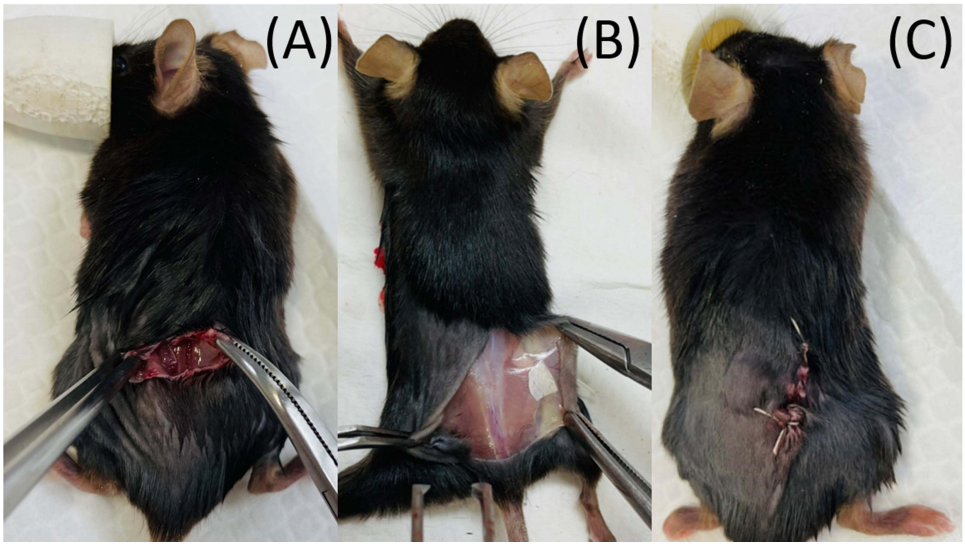

Figure 1 Experimental procedure for the implantation of the imiquimod/metronidazole-eluting membranes. (**A**) A cut was made on the mice's backs to expose the tissues, (**B**) implantation of the nanofibers, and (**C**) closure of the wound.

Small tissue samples from the area near the nanofibrous imiquimod/metronidazole membranes were collected on days 1, 3, 7, 14, 21, and 28 post-surgery (n=3). In vivo drug release was analyzed using HPLC. Additionally, six mice implanted with drug-loaded nanofibers were euthanized on days 1 and 3 post-surgery for histological analysis and blood sampling.

Therapeutic Animal Model of Drug-Eluting Nanofibers

On day 0, eight-week-old female C57BL/6 mice were inoculated with 1×10^6 cells per mouse, and the cells were dissolved in normal saline to a total volume of 100 μL through subcutaneous (S.C.) on the right flank back. On day 12, the mice were then divided into three groups (Figure 1B). The first group was the untreated control (tumor group). Mice in the second group received the implantation of pristine PLGA nanofibers under the tumor side, while the animals in the third group were implanted with imiquimod and metronidazole loaded nanofibers. Tumor volumes were assessed on days 7, 14, 21, and 28 by measuring with a caliper and calculating using the formula: length × (width) 2×0.5. Mice were euthanized if the tumor diameter exceeded 2 cm. On day 22, the mice were euthanized through carbon dioxide (CO_2) exposure, and the relevant splenocytes were collected for ELISA assay.

IFN-γ Production by Splenocyte Treated With HPV16 E7 hMC-I and II Peptide

On day 22, spleens were collected, and a single-cell suspension of splenocytes was generated. Four million splenocytes were exposed to 10 μg/mL of HPV16 E7 MHC-I and II peptide in a 2 mL volume of RPMI-1640 media supplemented with 10% fetal calf serum. These splenocytes were cultured in 24-well plates for 24 and 72 hours, after which the culture medium was collected. The concentration of IFN-γ was quantified using an ELISA assay in San Diego, CA, USA.

ELISA Assay

Supernatants were collected from the mice splenocyte after treated with E6 and E7 peptides for 24 and 72 hrs, respectively. Samples were stored at –20 °C prior to analysis of mouse IFN-γ through ELISA assay, which was performed according to the manufacturer's instructions (San Diego, CA, USA).

In vivo Fluorescence Imaging With the IVIS Spectrum System

To determine the expression of TC-1/luciferase tumor cells in the tumor-bearing mice, we performed in vivo fluorescence imaging using Vieworks Clevue imaging system on day 7, 14, 21, 28. Mice were injected intraperitoneally (i.p.) with D-Luciferin at a dose of 75 mg/kg body weight (200ul/mouse) and anesthetized with isoflurane. Briefly, the mice were anesthetized and placed onto the warm imaging stage of the IVIS apparatus subcutaneous position (right flank back) with continuous exposure to 1–2% isoflurane. Images were captured for 5–10 min after D-luciferin injection using the IVIS Imaging System (Xenogen, Alameda, CA). The photons emitted from the tumor side and its surroundings were quantified as total photon counts using Living Image 2.50 Software (Xenogen).

Statistical Analysis

Data are presented as the mean ± standard error of the mean (SEM) deviation. Data analysis was performed by using GraphPad Prism 6.01 software (GraphPad Software, Inc). Experiments statistical significance was determined using one-way ANOVA with the Bonferroni post hoc test. A p-values < 0.05 was considered significant. $*P < 0.05$, $**P < 0.01$, $***P < 0.001$.

Results

Assessment of Electrospun Nanofibers

Using the electrospinning technique, we successfully fabricated biodegradable nanofibrous mats. Figure 2 illustrates the microimages and fiber size distributions of both spun pure PLGA and PLGA nanofibrous membranes loaded with imiquimod/metronidazole. The 6:1 and 4:1 polymer-to-drug ratio nanofibrous membranes exhibited comparable fiber size distribution (188±56 nm and 210±77 nm, respectively) (p>0.05). However, these drugs embedded nanofibers displayed

 https://doi.org/10.2147/IJN.S482290

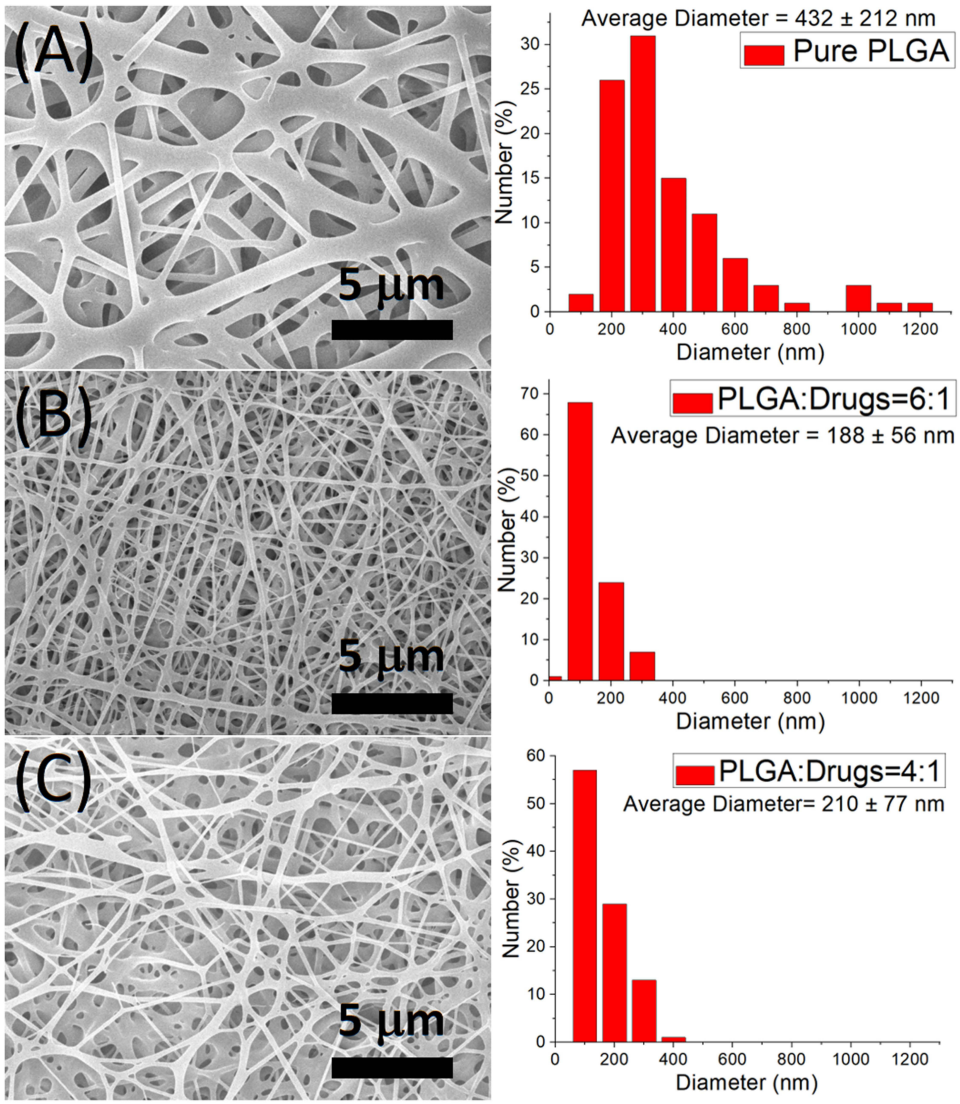

Figure 2 SEM microimages and fiber size distributions of (**A**) pure PLGA, (**B**) 6:1 and (**C**) 4:1 polymer-to-drug ratio nanofibers.

inferior size distribution to the pristine PLGA nanofibers (432±212 nm). This could be attributed to the reduction in polymer materials within the bulk as the drugs were added. Typically, a solution with lower polymer content has lower viscosity and is therefore more readily extended under the same electric force. Consequently, the fiber sizes of the drug-loaded nanofibers lessened accordingly.

The water contact angle measurements depicted in Figure 3 indicate a decrease in contact angles with the increasing content of pharmaceuticals in the mat (127.0°, 91.1°, and 70.9°, respectively, for the pure PLGA nanofibers and nanofibers with 6:1 and 4:1 polymer-to-drug ratios). Both imiquimod and metronidazole are water-soluble drugs, their presence thus promotes the hydrophilicity of spun nanofibers.

The tensile test findings presented in Figure 4 demonstrate a reduction in both ultimate strengths and elongations at the break of electrospun fibers as the content of incorporated imiquimod/metronidazole increases. This might be owing to the fact that the inclusion of drugs reduced the polymer percentage in the nanofibrous membranes. Electrospun nanofibers possessed less strength to resist the external stretching force due to electric field. Consequently, the estimated tensile strengths were compromised.

FTIR spectroscopy assay was completed to testify the added pharmaceuticals in the electrospun nanofibers. The assessed data in Figure 5 showed that the absorbances at 2970 and 1400–1450 cm^{-1}, corresponding to the vibration of

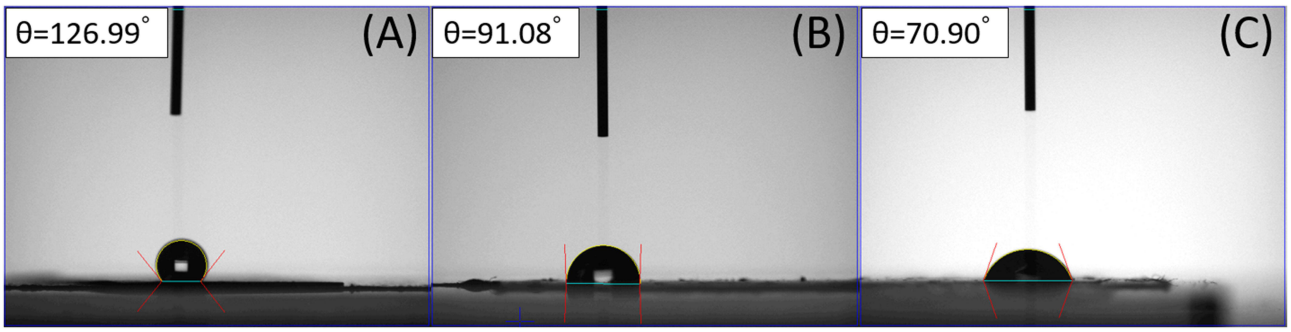

Figure 3 Water contact angles of (**A**) pure PLGA nanofibers, and (**B**) 6:1 and (**C**) 4:1 polymer-to-drug ratio nanofibers.

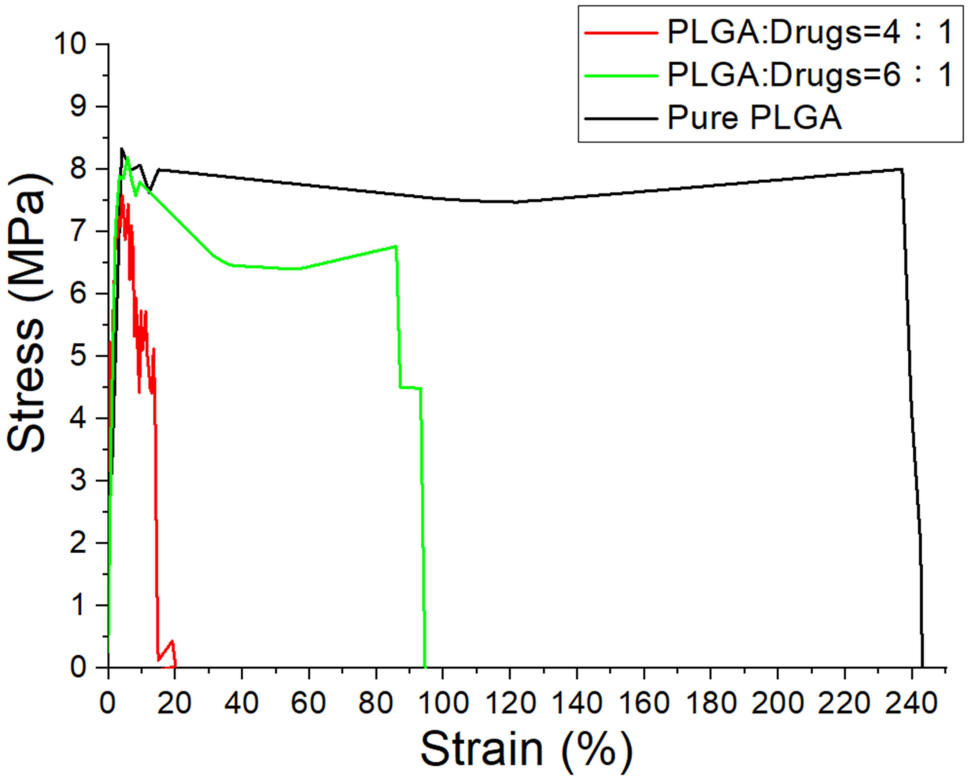

Figure 4 Tensile properties of spun nanofibers.

C-H bonds, diminished owing to the decrease of polymer content in the matrix by the addition of drugs. Meanwhile, the peaks near 1750 and 1100 cm^{-1}, corresponding to the C-H bonds, were also lessened due to the reduction of PLGAs in the nanofibers. More importantly, the new peaks at near 1620 cm^{-1} and 1530 cm^{-1} could be resulted from the vibrations of N-H and N-O and bonds from metronidazole and imiquimod,[24,25] respectively. Based on the FTIR spectra, we confirm that metronidazole and imiquimod have been successfully incorporated in the spun nanofibers.

In vitro Liberation Behavior of Imiquimod and Metronidazole

The in vitro daily and cumulative liberation patterns of imiquimod are displayed in Figure 6A and B, respectively, while Figure 7A and B show the daily and cumulative release profiles of metronidazole from the nanofibers, respectively. All pharmaceuticals showed a burst discharge at day 1, followed by a steady and nearly first-order drug release pattern through 30 days. The daily release characteristics were similar for both drug-eluting nanofibers with varying drug loadings, except some tiny second peak releases were noted for imiquimod with 4:1 ratio. The nanofibers generally

https://doi.org/10.2147/IJN.S482290

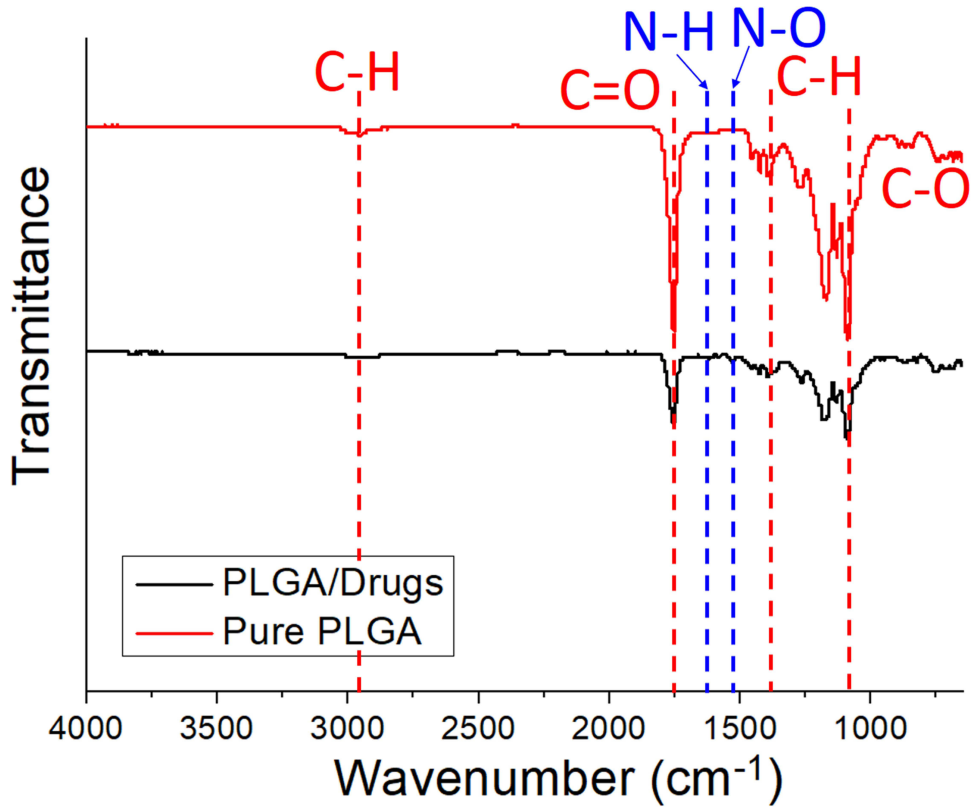

Figure 5 FTIR spectra of pure PLGA and imiquimod/metronidazole loaded PLGA nanofibers.

showed a minor deviation of the release curves, suggesting that the drugs were uniformly incorporated in the spun nanofibrous mats. While the nanofibers released approximately 60% of imiquimod in 30 days, they discharged nearly 90% of totally loaded metronidazole at the same time. This might be due to the fact that metronidazole is a water-soluble drug and can be easily dissolved by the PBS. The release rate of metronidazole was thus superior to that of imiquimod. In sum, all drug-eluting nanofibrous mats could discharge high levels of imiquimod and metronidazole for more than 30 days in vitro.

In vivo Release

The investigation also encompassed an assessment of in vivo drug release dynamics. The plotted data in Figure 8 delineate that the drug-embedded nanofibrous membranes exhibited sustained release of imiquimod and metronidazole over a span of four weeks. Notably, the concentration of the drugs detected in the plasma was notably lower compared to that observed at the target site.

Histology Analysis

Histological images from each time point (postoperative days 1, 2, and 3) are depicted in Figure 9. No signs of inflammation such as elevated leukocytes or tissue necrosis were found in the histological assay of any samples.

Engineering Imiquimod-Loaded PLGA Treatment Alleviates Tumor Growth and Enhances Th1 Cytokine Production

TC1 cells inoculated into the C57BL/6 mice and treatment protocol as described in Figure 10A. All mice were started to form a tumor 7 days after TC1 tumor cells transplanted. Tumor was continually growing in the control and PLGA group from day 14 to day 21. Mice after receiving imiquimod-loaded PLGA treatment have significantly decreased the tumor size in Figure 10A and B. Moreover, TC1 tumor cells could stably express the luciferase gene, when we subcutaneously

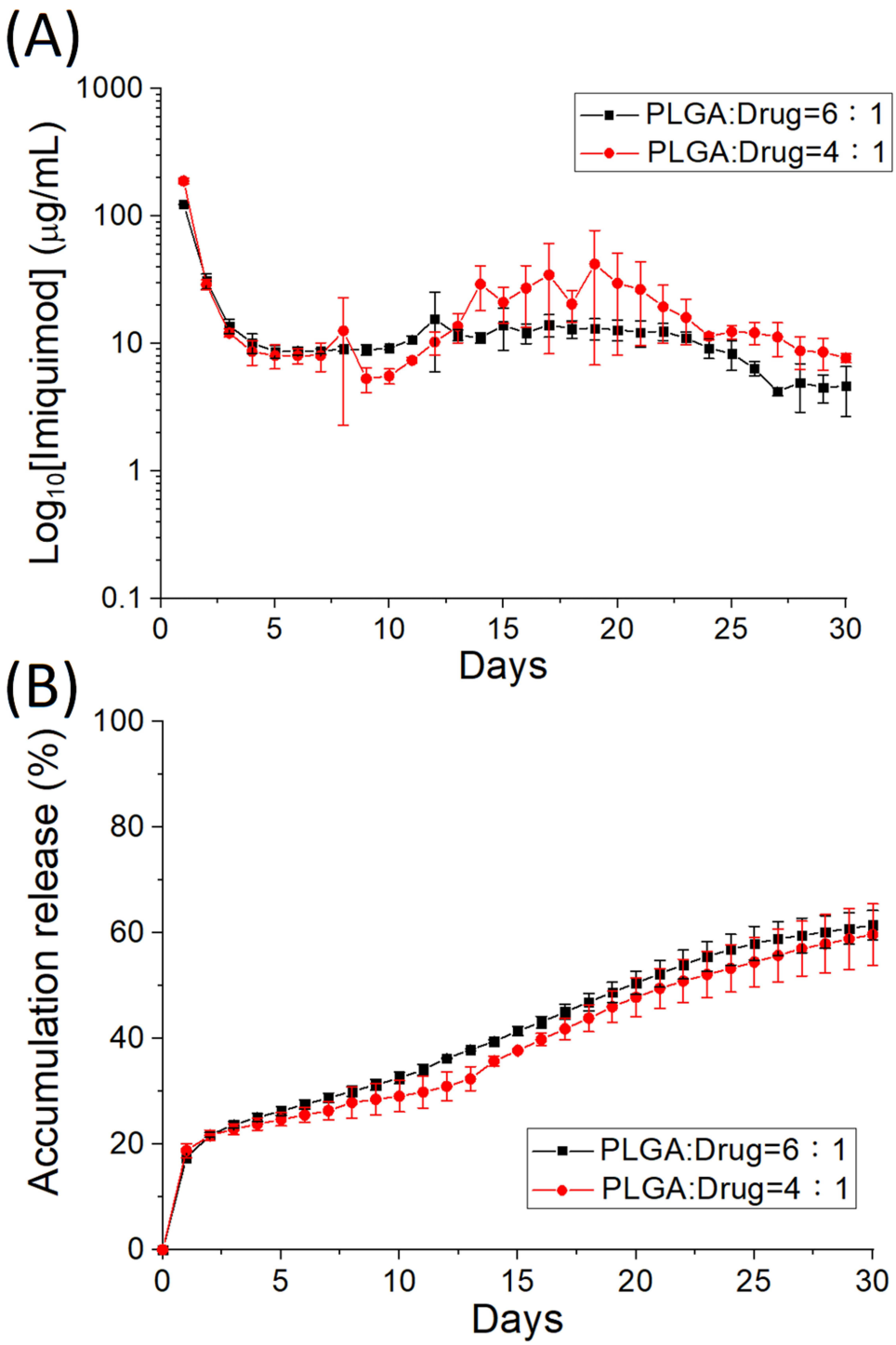

Figure 6 In vitro (**A**) daily and (**B**) cumulative discharge of imiquimod from the nanofibers.

injected these cells into the mice. As the tumor grew, the luminescence intensity of these cells was captured by the IVIS imaging system both visually and quantitatively. Measurement of tumor volume and the luminescence intensity were both appropriate for assess the tumor progression and regression. In Figure 10C and D, as the tumor grew, implantation of PLGA/IM group reduced the luminescence intensity both visually and quantitatively compared with the control and PLGA groups. According to previous studies, IFN-γ was play a role in tumor regression.[26,27] We assessed the expression of IFN-γ on splenocytes following re-stimulation with 10 μg/mL HPV16 E7 MHC-I and II peptides for 24 and 72h

https://doi.org/10.2147/IJN.S482290

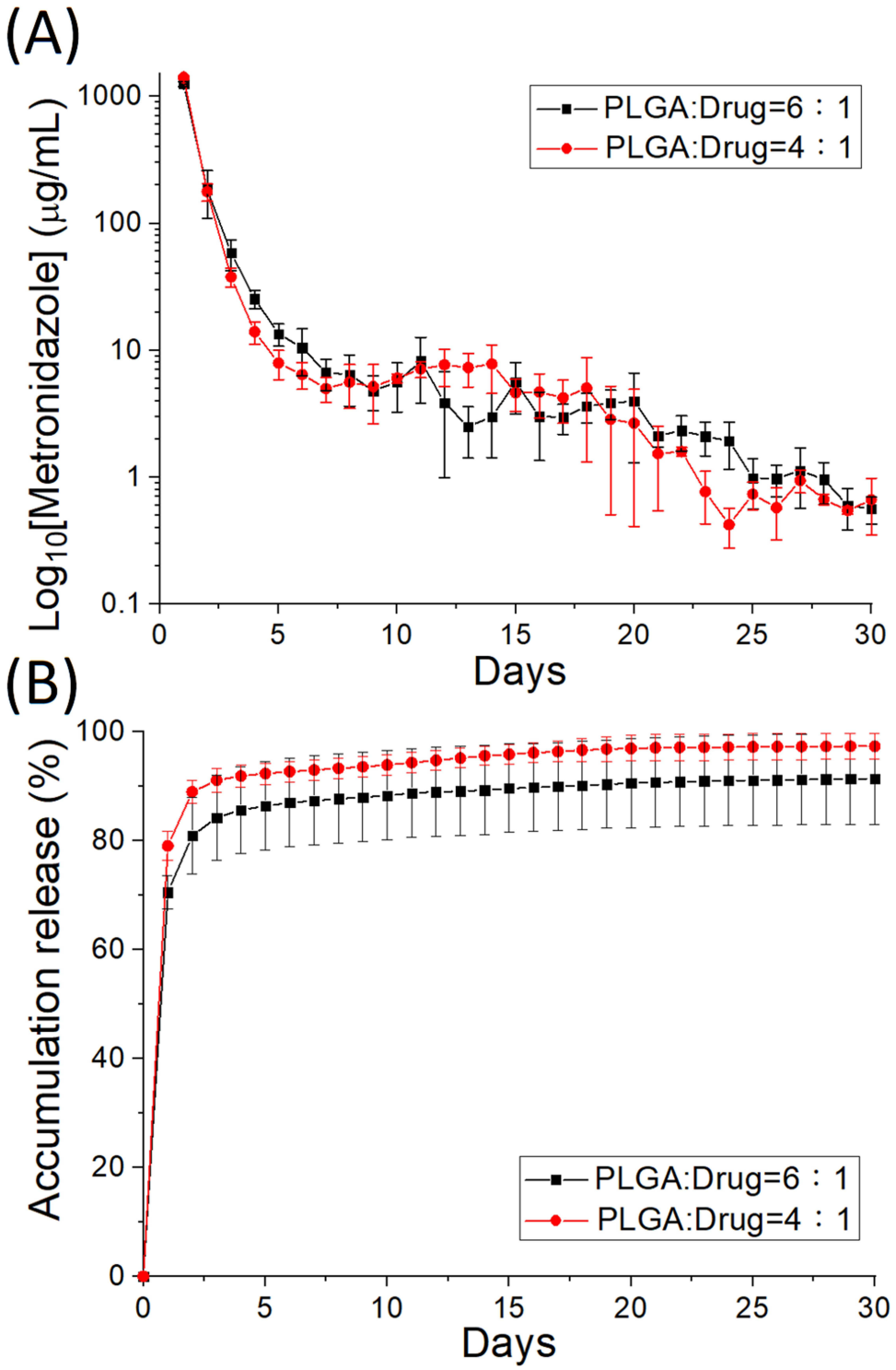

Figure 7 In vitro (**A**) daily and (**B**) cumulative discharge of metronidazole from the nanofibers.

(Figure 10E) and we found that we implanted mice with PLGA/IM had significantly increased IFN-γ production. In contrast, tumor control and PLGA only showed a lower expression of IFN-γ. Taken together, we demonstrated that the fabricated biodegradable imiquimod-loaded PLGA membrane was capable of regressing tumor growth and enhancing Th1 cytokine production.

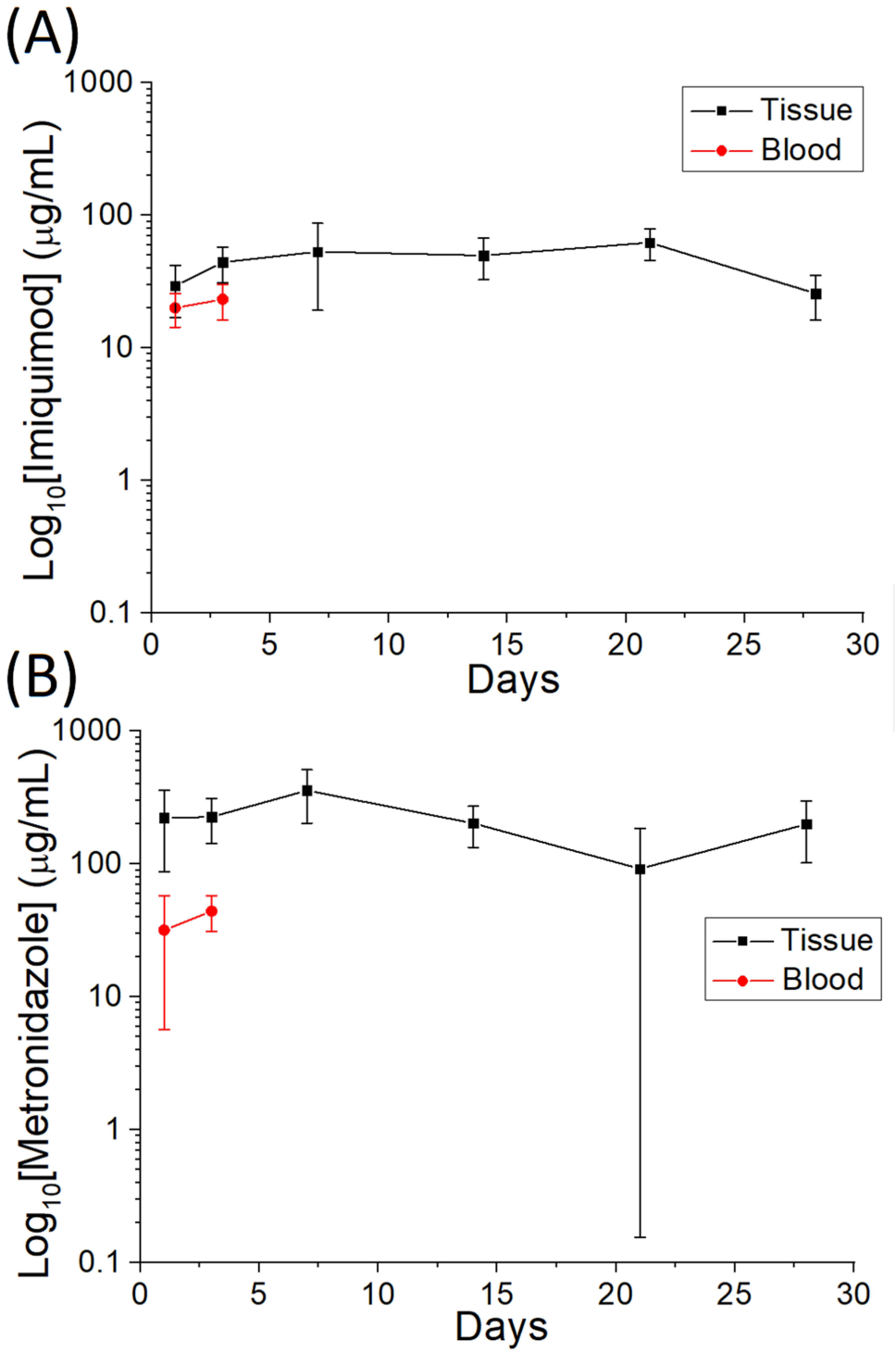

Figure 8 In vivo drug concentrations of (**A**) imiquimod and (**B**) metronidazole at the targeted tissue and in the plasma.

Discussion

Advanced cervical carcinoma is a leading cause of mortality, with a high death rate. The majority of cases are attributed to human papillomavirus (HPV) infection, despite the availability of prophylactic vaccines. Treating cervical carcinoma remains challenging.[28] The high mortality may be attributed to the fact that most cases are diagnosed at an advanced stage. Metastatic cervical cancers have a 5-year survival rate of around 50%. Various treatments, including chemotherapy, radiotherapy, and immunotherapy, are used to manage advanced stage cervical cancers. However, treatment may fail

https://doi.org/10.2147/IJN.S482290

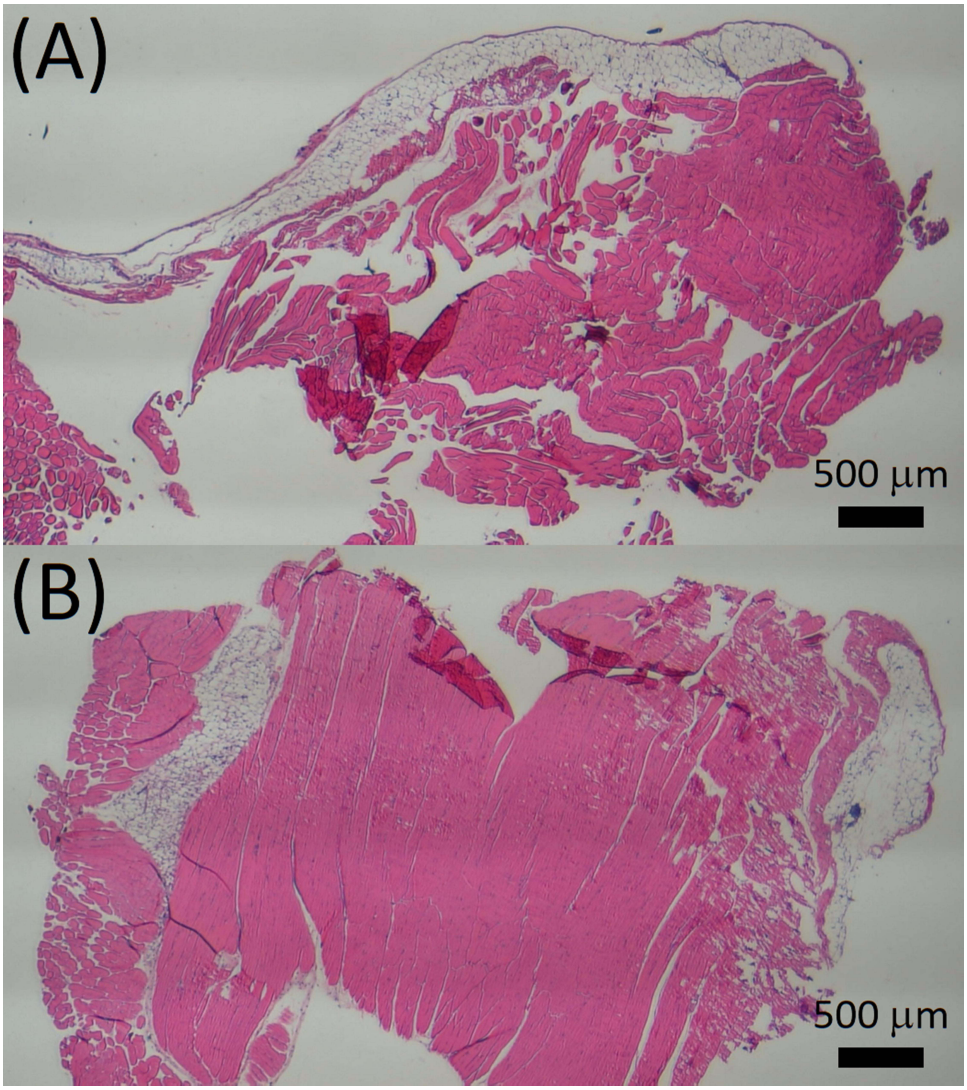

Figure 9 Histological analysis images at (**A**) day 1 and (**B**) day 3.

resulted from drug resistance and/or rapid tumor progression. Additionally, anticancer treatments may cause adverse effects from the drugs, limiting the use of high drug doses. Therefore, there is a critical need for improved diagnosis and treatment of cervical cancers to enhance survival rates.[29]

The cervical epithelium typically serves as a natural barrier against HPV infection.[30,31] However, conventional cervical screening methods, such as Pap smear and biopsy, may inadvertently damage the cervical epithelium. Moreover, treatments for cervical intraepithelial neoplasia (CIN), including laser therapy and cervical conization, also result in epithelial destruction. Consequently, there is a need for local agents to fortify the barrier against iatrogenic cervical lesions and avoid subsequent HPV infections.

The advance of nanotechnology has provided a promising approach to revolutionize cancer management, offering innovative strategies for cancer treatment. Research has explored various targeted drug delivery systems to enhance the cumulation of anti-tumor medications at carcinoma sites. In the realm of cervical cancer, nanotechnology is increasingly being explored to enhance early diagnosis and improve the efficacy of vaccines and treatments.[32]

In this study, biodegradable PLGA nanofibrous membranes were developed to facilitate the sustained delivery of imiquimod and metronidazole to the targeted tumor site for treating cervical cancers. Nanofibers, with their high surface area-to-volume ratio, provide an effective route for delivering drugs that are insoluble in water or have poor water

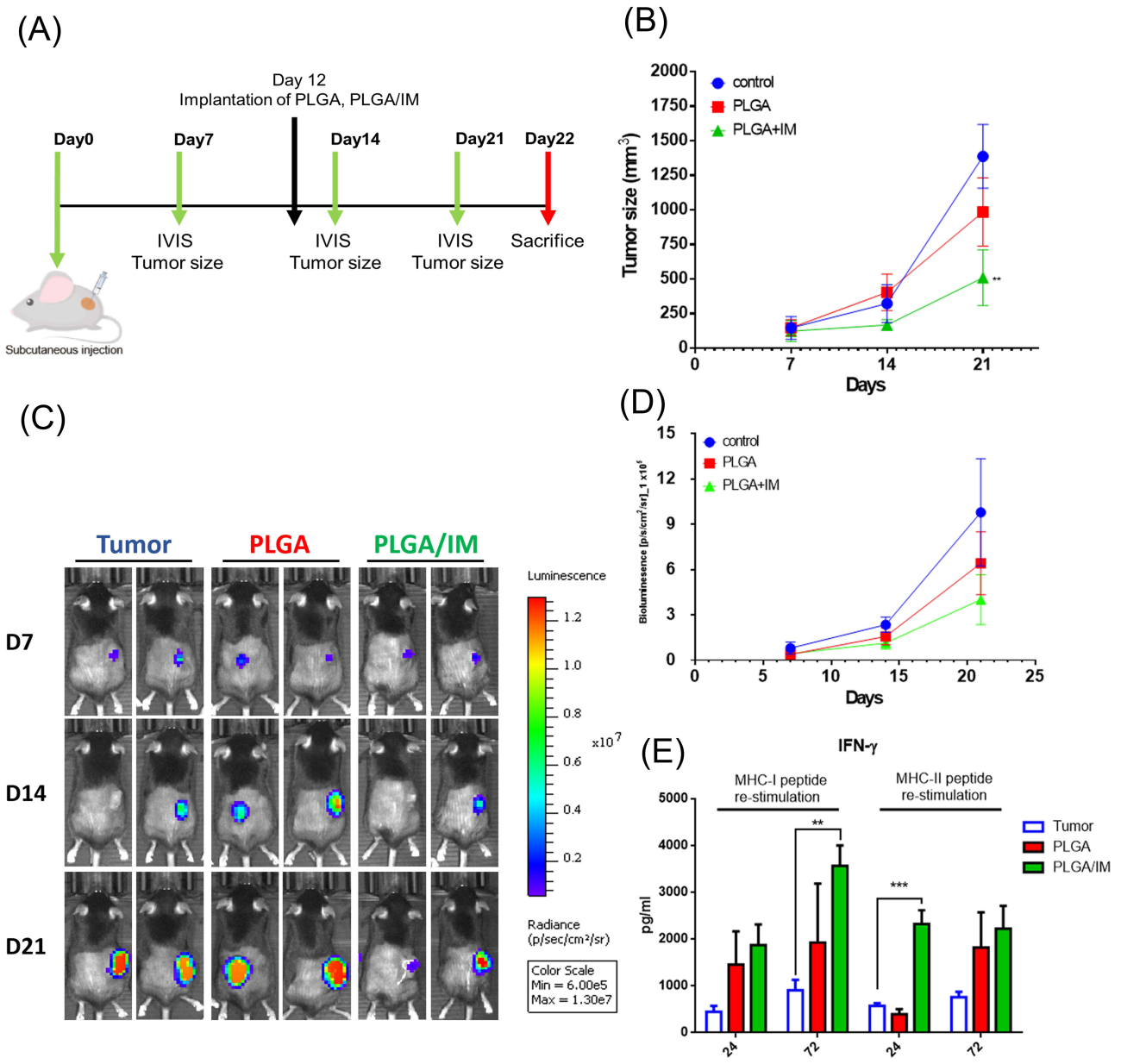

Figure 10 Effect of the PLGA nanofiber with imiquimod treatments on TC1-luc subcutaneous tumor model.TC1-luc tumor-bearing model as described in (**A**): On day 0, mice were subcutaneous injection with 100 μL of 1×10^6 tumor cells on the back. On day 12, mice were subcutaneous implantation of PLGA and PLGA/IM nanofiber under the tumor side by surgery. On days 7, 14, 21, 28, mice were measured the tumor volume once a week using caliper and calculated according to the formula: length × (width) 2×0.5. On Day 22, the mice were euthanized by using carbon dioxide (CO_2). (**B**) Tumor volume was calculated once a week. (**C**) IVIS images were obtained once a week after subcutaneous inoculation of TC1-luc cells for total 3 weeks. (**D**) Luminescent intensity of photons emitted from the tumor side in the images was quantified. (**E**) Increased IFN-γ production, as determined by ELISA, culture medium from splenocyte after treated HMC-I and MHC-II peptides for 24, 74 hours. Data are expressed as mean ± S.E.M (n ≧ 4). ** $P < 0.01$, *** $P < 0.001$, as compared with the control and PLGA/IM group.

solubility. Electrospun drug-loaded nanofibers not only exhibit microscopic-scale dimensionality but also possess macroscopic form. This unique characteristic provides drug-loaded nanofibers with the advantages of nano-scale drug delivery systems in altering the biopharmaceutical and/or pharmacokinetic properties of the drug molecule to expected therapeutical outcomes.[33–35]

Numerous biomaterials have been investigated for delivering pharmaceuticals, genes, and peptides. Among these, PLGA is a widely used biodegradable polymer in drug delivery systems. Its popularity stems from its versatility, biocompatibility, and tunable degradation properties.[36,37] Local drug delivery using PLGA offers a promising approach

https://doi.org/10.2147/IJN.S482290

for targeted and sustained release of therapeutic agents at specific sites within the body, designed to administer medications directly to localized regions, such as tumors, while minimizing systemic exposure and associated side effects.

In general, the drug release from a pharmaceutical-incorporated degradable implant occurs in three stages, each identified by burst discharge, diffusion-controlled elution, or degradation-governed release.[38] During electrospinning, the majority of the incorporated drugs are confined in the volumes of the PLGA fibers. However, a fraction of the drug is deposited on the exterior of the nanofibrous mats, resulting in the initial burst. After the burst, the release pattern is governed by diffusion and material degradation simultaneously. Thus, a few tiny peak releases might be observed for imiquimod (a less water-soluble drug) after the burst at various days; thereafter, the drug elution profiles displayed gradual decreases. In contrast, the nanofibrous membranes discharged the highly water-soluble metronidazole evenly after the initial burst.

The empirical data illustrated that the imiquimod/metronidazole-eluting nanofibers display a sustained drug release pattern in vitro through 30 days, with some minor peak releases noted. During the 28-day period in vivo, drug levels remained consistently high at the target site, while remaining significantly lower in the bloodstream. Imiquimod, a Toll-like receptor-7/8 agonist, provides a bridge for innate immunity and adaptative immunity. It could stimulate the synthesis of various cytokines (IFN-α, IFN-γ, TNF-α, IL-1a, IL-2, IL-6, IL-8, IL-10, IL-12, G-CSF, and GM-CSF) via macrophages and DC, skewing naïve T cell differentiation towards a Th1 phenotype, enhancing the anti-tumoral immunity, especially IFN-γ. Importantly, the animal tests demonstrated that the degradable drug-loaded nanofibrous mats offer sustainable release of imiquimod and metronidazole for four weeks in vivo. This prolonged release of therapeutic concentrations of imiquimod and metronidazole offers specific advantages for managing cervical cancers and preventing their recurrence.

Despite the demonstrated efficacy of the imiquimod/metronidazole-embedded nanofibers, this study encountered several limitations. Firstly, the study enrolled a relatively small number of animals, limiting the robustness of the findings. Secondly, the relevance of our findings to human cervical carcinoma cases remains unclear. Transitioning from animal trials to human trials for imiquimod/metronidazole-embedded nanofibers involves a series of critical steps to ensure safety, efficacy, and regulatory compliance, all of which warrant further investigation.

Conclusions

We successfully developed degradable nanofibrous mats capable of eluting imiquimod and metronidazole, using poly[(d, l)-lactide-co-glycolide] (PLGA) as the carrier matrix. The in vitro and in vivo drug release profiles of these nanofibers were evaluated. In vitro release of imiquimod and metronidazole was analyzed using HPLC, while in vivo release was assessed in an animal model. Our experimental findings demonstrated sustained release of effective concentrations of both drugs for over four weeks post-surgery, with minimal systemic drug levels detected in the blood. Histological analysis also indicated no significant inflammation. These results suggest that nanofibers enabling sustained release of imiquimod and metronidazole show potential for cervical cancer treatment.

Funding

Financial support for this research was provided by the National Science and Technology Council, Taiwan (Contract No. 111-2221-E-182-005-MY2) and Chang Gung Memorial Hospital-Linkou (Contract No. CMRPD2P0071, CMRPD2M0132, CMRPG2L0321, CMRPG2L0322).

Disclosure

The authors declare no conflicts of interest with respect to this work.

References

1. Burmeister CA, Khan SF, Schafer G, et al. Cervical cancer therapies: current challenges and future perspectives. *Tumour Virus Res*. 2022;13:200238. doi:10.1016/j.tvr.2022.200238
2. Santoro A, Inzani F, Angelico G, et al. Recent advances in cervical cancer management: a review on novel prognostic factors in primary and recurrent tumors. *Cancers*. 2023;15(4):1137. doi:10.3390/cancers15041137
3. Pang SS, Murphy M, Markham MJ. Current management of locally advanced and metastatic cervical cancer in the United States. *JCO Oncol Pract*. 2022;18(6):417–423. doi:10.1200/OP.21.00795

4. Choi S, Ismail A, Pappas-Gogos G, Boussios S. HPV and cervical cancer: a review of epidemiology and screening uptake in the UK. *Pathogens*. 2023;12(2):298. doi:10.3390/pathogens12020298
5. Perkins RB, Wentzensen N, Guido RS, Schiffman M. Cervical cancer screening: a review. *JAMA*. 2023;330(6):547–558. doi:10.1001/jama.2023.13174
6. Burd EE. Human papillomavirus and cervical cancer. *Clin Microbiol Rev*. 2023;16(1):1–17. doi:10.1128/CMR.16.1.1-17.2003
7. Massobrio R, Bianco L, Campigotto B, et al. New frontiers in locally advanced cervical cancer treatment. *J Clin Med*. 2024;13(15):4458. doi:10.3390/jcm13154458
8. Liontos M, Kyriazoglou A, Dimitriadis I, Dimopoulos M-A, Bamias A. Systemic therapy in cervical cancer: 30 years in review. *Crit Rev Oncol Hematol*. 2019;137:9–17. doi:10.1016/j.critrevonc.2019.02.009
9. Monk BJ, Enomoto T, Kast WM, et al. Integration of immunotherapy into treatment of cervical cancer: recent data and ongoing trials. *Cancer Treat Rev*. 2022;106:102385. doi:10.1016/j.ctrv.2022.102385
10. Ma Y, Wang X, Zong S, et al. Local, combination chemotherapy in prevention of cervical cancer recurrence after surgery by using nanofibers co-loaded with cisplatin and curcumin. *RSC Adv*. 2015;5(129):106325–106332. doi:10.1039/C5RA17230F
11. Zhang Z, Wu Y, Kuang G, et al. Pt(IV) prodrug-backboned micelle and DCA loaded nanofibers for enhanced local cancer treatment. *J Mater Chem B*. 2017;5(11):2115–2125. doi:10.1039/C7TB00178A
12. Zhang ZY, Liu S, Qi YX, et al. Time-programmed DCA and oxaliplatin release by multilayered nanofiber mats in prevention of local cancer recurrence following surgery. *J Control Release*. 2016;235:125–133. doi:10.1016/j.jconrel.2016.05.046
13. Chen YP, Liu YW, Lee D, Qiu JT, Lee TY, Liu SJ. Biodegradable andrographolide-eluting nanofibrous membranes for the treatment of cervical cancer. *Int J Nanomed*. 2019;14:421–429. doi:10.2147/IJN.S186714
14. Wagstaff AJ, Perry CM. Topical imiquimod: a review of its use in the management of anogenital warts, actinic keratoses, basal cell carcinoma and other skin lesions. *Drugs*. 2007;67(15):2187–2210. doi:10.2165/00003495-200767150-00006
15. Gupta AK, Browne M, Bluhm R. Imiquimod: a review. *J Cutan Med Surg*. 2002;6(6):554–560. doi:10.1177/120347540200600607
16. Dockrell DH, Kinghorn GR. Imiquimod and resiquimod as novel immunomodulators. *J Antimicrob Chemother*. 2001;48:751–755. doi:10.1093/jac/48.6.751
17. Hamar B, Teutsch B, Hoffmann E, et al. Imiquimod is effective in reducing cervical intraepithelial neoplasia: a systematic review and meta-analysis. *Cancers*. 2024;16(8):1610. doi:10.3390/cancers16081610
18. Freeman CD, Klutman NE, Lamp KC. Metronidazole: a therapeutic review and update. *Drugs*. 1997;54(5):679–708. doi:10.2165/00003495-199754050-00003
19. Leitsch D. A review on metronidazole: an old warhorse in antimicrobial chemotherapy. *Parasitology*. 2019;146(9):1167–1178. doi:10.1017/S0031182017002025
20. Kao CW, Lee D, Wu MH, Chen JK, He HL, Liu SJ. Lidocaine/ketorolac loaded biodegradable nanofibrous anti-adhesive membranes that offer sustained pain relief for surgical wounds. *Inter J Nanomed*. 2017;12:5893–5901. doi:10.2147/IJN.S140825
21. Paula DD, Martins CA, Bentley MVLB. Development and validation of HPLC method for imiquimod determination in skin penetration studies. *Biomed Chromatogr*. 2008;22(12):1416–1423. doi:10.1002/bmc.1075
22. Salvesen B, Leinebo O, Bergan T. Assay of metronidazole by HPLC compared with microbial method. *Scand J Gastroenterol Suppl*. 1984;91:31–43.
23. Lhotakova K, Grzelak A, Polakova I, Vackova J, Smahel M. Establishment and characterization of a mouse tumor cell line with irreversible downregulation of MHC class I molecules. *Oncol Rep*. 2019;42(6):2826–2835. doi:10.3892/or.2019.7356
24. Carneiro RL, Poppi RJ. Infrared imaging spectroscopy and chemometric tools for in situ analysis of an imiquimod pharmaceutical preparation presented as cream. *Spectrochim Acta A Mol Biomol Spectrosc*. 2014;118:215–220. doi:10.1016/j.saa.2013.08.104
25. Ashtarinezhad A, Shirazi FH, Vatanpour H, Mohamazadehasl B, Panahyab A, Nakhjavani M. FTIR-microspectroscopy detection of metronidazole teratogenic effects on mice fetus. *Iran J Pharm Res*. 2014;13(Suppl):101–111.
26. Jorgovanovic D, Song M, Wang L, Zhang Y. Roles of IFN-γ in tumor progression and regression: a review. *Biomarker Res*. 2020;8(1):49. doi:10.1186/s40364-020-00228-x
27. Gocher AM, Workman CJ, Vignali DAA. Interferon-γ: teammate or opponent in the tumour microenvironment? *Nat Rev Immunol*. 2022;22(3):158–172. doi:10.1038/s41577-021-00566-3
28. Lin CC, Tsai CC, Lee JM, et al. The efficacy of a novel vaccine approach using tumor cells that ectopically express a codon-optimized murine GM-CSF in a murine tumor model. *Vaccine*. 2016;34:134–141. doi:10.1016/j.vaccine.2015.10.106
29. McKee SJ, Bergot A-S, Leggatt GR. Recent progress in vaccination against human papillomavirus-mediated cervical cancer. *Rev Med Virol*. 2015;25:54–71. doi:10.1002/rmv.1824
30. Chen J. Signaling pathways in HPV-associated cancers and therapeutic implications. *Rev Med Virol*. 2015;25:24–53. doi:10.1002/rmv.1823
31. Wong IY, Bhatia SN, Toner M. Nanotechnology: emerging tools for biology and medicine. *Gene Dev*. 2013;27:2397–2408. doi:10.1101/gad.226837.113
32. Chen J, Gu W, Yang L, et al. Nanotechnology in the management of cervical cancer. *Rev Med Virol*. 2015;25:72–83. doi:10.1002/rmv.1825
33. Yu D-G, Zhu L-M, White K, Branford-White C. Electrospun nanofiber-based drug delivery systems. *Health*. 2009;1(2):67–75. doi:10.4236/health.2009.12012
34. Kajdic S, Planinsek O, Gasperlin M, Kocbek P. Electrospun nanofibers for customized drug-delivery systems. *J Drug Deliv Sci Technol*. 2019;51:672–681. doi:10.1016/j.jddst.2019.03.038
35. Torres-Martinez EJ, Bravo JMC, Medina AS, Gonzalez GLP, Gomez LJV. A summary of electrospun nanofibers as drug delivery system: drugs loaded and biopolymers used as matrices. *Curr Drug Deliv*. 2018;15(10):1360–1374. doi:10.2174/1567201815666180723114326
36. Makadia K, Siegel SJ. Poly lactic-*co*-glycolic acid (PLGA) as biodegradable controlled drug delivery carrier. *Polymers*. 2011;3(3):1377–1397. doi:10.3390/polym3031377
37. Gentile P, Chiono V, Carmagnola I, Hatton PV. An overview of poly(lactic-co-glycolic) acid (PLGA)-based biomaterials for bone tissue engineering. *Int J mol Sci*. 2014;15(3):3640–3659. doi:10.3390/ijms15033640
38. Liu KS, Kao CW, Tseng YY, et al. Assessment of antimicrobial agents, analgesics, and epidermal growth factors-embedded anti-adhesive poly (lactic-co-glycolic acid) nanofibrous membranes: in vitro and in vivo studies. *Int J Nanomed*. 2021;16:4471–4480. doi:10.2147/IJN.S318083